HHS Public Access

Author manuscript

Brain Res. Author manuscript; available in PMC 2016 June 03.

Published in final edited form as:

Brain Res. 2015 August 7; 1616: 45–57. doi:10.1016/j.brainres.2015.04.052.

Structural–functional coupling changes in temporal lobe epilepsy

Sharon Chiang[a,1], **John M. Stern**[b], **Jerome Engel Jr.**[b,c,d,e], and **Zulfi Haneef**[f,g,*,1]

[a]Department of Statistics, Rice University, Houston, TX, USA

[b]Department of Neurology, University of California, Los Angeles, CA, USA

[c]Department of Neurobiology, University of California, Los Angeles, CA, USA

[d]Department of Psychiatry and Biobehavioral Sciences, University of California, Los Angeles, CA, USA

[e]The Brain Research Institute, University of California, Los Angeles, CA, USA

[f]Department of Neurology, Baylor College of Medicine, Houston, TX, USA

[g]Neurology Care Line, VA Medical Center, Houston, TX, USA

Abstract

Alterations in both structural connectivity (SC) and functional connectivity (FC) have been reported in temporal lobe epilepsy (TLE). However, the relationship between FC and SC remains less understood. This study used functional connectivity MRI and diffusion tensor imaging to examine coupling of FC and SC within the limbic network of TLE, as well as its relation to epilepsy duration, regional changes, and disease laterality in 14 patients with left TLE, 10 with right TLE, and 11 healthy controls. Structural and functional networks were separately constructed and the correlation estimated between structural and functional connectivity. This measure of SC–FC coupling was compared between left/right TLE and controls, and correlated with epilepsy duration. Elastic net regression was used to investigate regional structural and functional changes associated with SC–FC coupling. SC–FC coupling was decreased in left TLE compared to controls, and accompanied by reductions in FC for left and right TLE and in SC for left TLE. When examined in relation to disease duration, an increase in SC–FC coupling with longer epilepsy duration was observed, associated predominantly with structural loss of the fusiform and frontal inferior orbital gyrus in left TLE and functional hub redistribution in right TLE. These results suggest that decoupling between structural and functional networks in TLE is modulated by several factors, including epilepsy duration and regional changes in the fusiform, frontal inferior orbital gyrus, posterior cingulate, and hippocampus. SC–FC coupling may provide a more sensitive biomarker of disease burden in TLE than biomarkers based on single imaging modalities.

[*]Correspondence to: Peter Kellaway Section of Neurophysiology, Department of Neurology, Baylor College of Medicine, One Baylor Plaza, MS: NB302, Houston, TX 77030, USA. Fax: +1 713 798 7561. ; Email: zulfi.haneef@bcm.edu (Z. Haneef)

[1]Both authors contributed equally to this work.

Appendix A. Supporting information

Supplementary data associated with this article can be found in the online version at http://dx.doi.org/10.1016/j.brainres.2015.04.052.

Keywords

Functional magnetic resonance; imaging; Diffusion tensor imaging; Temporal lobe epilepsy; Elastic net; Connectomics; Limbic network

1. Introduction

Traditionally, a focal model of temporal lobe epilepsy (TLE) has evaluated single pathological regions as responsible for seizure generation. However, there is growing evidence supporting network models of TLE, as seizures are found to be associated with alterations in widespread networks involving bilateral temporal and extratemporal structures (Engel et al., 2013). Recent advances in neuroimaging have enabled the study of neurological diseases on a network level through the use of connectomics. This has led to considerable advances in understanding interactions between brain regions and groups of brain regions in network diseases such as TLE (Engel et al., 2013). The connectomic studies of TLE have tended to separately analyze structural and functional networks, and consideration of both forms of connectivity in combination may provide a more nuanced analysis (van Diessen et al., 2013).

Although a large number of structural and functional imaging studies have reported altered structural and functional connectivity in TLE, only a few studies have directly investigated the interplay between structural and functional connectivity networks in TLE (Liao et al., 2011; Voets et al., 2009). While structural connectivity (SC) is generally considered the substrate for functional connectivity (FC) (Greicius et al., 2009), a uniform and predictable relationship between SC and FC is not present and no consensus has been reached on the interaction between them (van Diessen et al., 2013; Zhu et al., 2013). The strength of FC need not be necessarily proportional to the strength of SC, as within stable SC frameworks there is reconfiguration of FC networks (Deco et al., 2011). Furthermore, FC may also exert an effect on SC through plasticity (Hagmann et al., 2010). Improved understanding of the relationship between SC and FC is necessary to improve our understanding of the pathophysiology underlying TLE. Additionally, development of more accurate bio-markers for the diagnostic or therapeutic options in TLE using integrative data models requires an understanding of how structural and functional data sources relate to each other.

The use of correlation estimates between subject-level resting-state fMRI and diffusion tensor imaging (DTI) connectivity matrices was proposed recently and allows for quantification of the agreement between structure and function (Skudlarski et al., 2008). This measure, known as SC–FC coupling, has demonstrated its potential for characterizing changes in structural–functional network relationships through other neurological disorders, including idiopathic generalized epilepsy (Zhang et al., 2011) and schizophrenia (van den Heuvel et al., 2013). SC–FC decoupling has been observed in other neurological diseases, including Alzheimer's disease (Sun et al., 2014) and idiopathic generalized epilepsy (Zhang et al., 2011). A previous study correlating DTI and task-based fMRI for individual regions has found that decoupling of structure and function within the arcuate fasciculus is greater in left than right TLE patients (Rodrigo et al., 2008). However, SC-FC coupling on a network

level has not been explored in TLE to our knowledge. Limbic regions are primarily involved with seizures in TLE (Avoli et al., 2002; Bertram et al., 1998), and may undergo altered structural and functional connectivity (Bonilha et al., 2012; Chiang et al., 2014; Concha et al., 2005). In this study, we employ the measure of SC-FC coupling to investigate the interaction between limbic structure and function in TLE on a network level. In particular, we examine: (1) how SC-FC coupling of the limbic network is affected in left and right TLE compared to healthy controls, (2) whether these network changes differ with TLE laterality, (3) whether SC-FC coupling is correlated with epilepsy duration, and (4) which regional changes in structure and function modulate SC-FC coupling changes.

2. Results

2.1. Groupwise comparison

Controls, left, and right TLE subgroups were similar with respect to gender, age, handedness, and education (Table 1 and Table 2). Non-parametric permutation testing revealed that limbic SC was decreased in left TLE (p=0.02) but unchanged in right TLE (p=0.27) (Fig. 3a), and that limbic FC was decreased in both left TLE (p=0.01) and right TLE (p<0.001) (Fig. 3b). SC-FC coupling was decreased in left TLE (0.1±70.06, p=0.02) and was non-significantly lower in right TLE (0.16 7 0.09, p=0.23) compared to controls (0.18±0.06) (Fig. 3c). In left TLE patients, pairwise FC strength was significantly decreased between the left posterior cingulate/ left hippocampus (p=0.02) and between the left thalamus/ right posterior cingulate (p=0.02). In right TLE patients, pairwise FC strength was significantly decreased between the left posterior cingulate/right hippocampus (p=0.04), right posterior cingulate/right parahippocampus (p=0.04), and left thalamus/right posterior cingulate (p=0.04). In contrast to FC, no significant changes in pairwise SC were observed. Taken together, the absence of SC change in right TLE and absence of observed pairwise SC changes suggest that FC is more affected than SC in TLE.

2.2. Correlation of SC-FC coupling with epilepsy duration

Correlation analysis demonstrated a trend toward a decrease in mean limbic FC with longer epilepsy duration (r=−0.39, p=0.07) (Fig. 3d). No significant change in mean limbic SC (r= +0.21, p=0.38) was observed. The directionality and non-significance of these estimates remained consistent after controlling for the effects of age, for both mean limbic FC (r= −0.24, p=0.29) and mean limbic SC (r=+0.21, p=0.38). An increase in SC-FC coupling was observed with longer TLE duration independent of age (p=0.02) (Fig. 3e), which was separately significant for both left (p=0.03) and right (p=0.046) TLE subgroups. Age had a positive association with SC-FC coupling (r=+0.43) and was controlled for in the association between epilepsy duration and SC-FC coupling, in order to control for potential confounding effects based on the change-in-estimate (CE) criterion (CE_{age}, 16.1%). The decrease in mean FC (CE_{FC}, 5.3%) had a greater effect than changes in mean SC ($CE_{S}C$, 0.032%) on the increase in SC-FC coupling with epilepsy duration.

2.3. Regional structural and functional factors in SC-FC coupling

Regional measures associated with SC-FC decoupling in TLE in more than 50% of elastic net (EN) cross-validation runs are shown in Table 3, with a conservative threshold of 50%

chosen in order to avoid missing relevant predictors (Bunea et al., 2011). Table 4 shows regional changes associated with SC-FC decoupling separately for left and right TLE subgroups.

Structural and functional changes of the hippocampus, posterior cingulate gyrus, and frontal inferior orbital gyrus had the highest probability of association with SC-FC decoupling in TLE (Table 3, Fig. 4). Structural and functional changes in the right fusiform, left frontal inferior orbital gyrus, bilateral posterior/left anterior cingulate gyrus, and left caudate contributed to SC-FC decoupling in left TLE, whereas functional changes in bilateral hippocampi contributed to SC-FC decoupling in right TLE (Table 4, Fig. 4). Regional changes identified as mediating the increase in SC-FC coupling with epilepsy duration included decreases of fractional anisotropy (FA) in the right fusiform gyrus and increases of mean diffusivity (MD) in the left frontal inferior orbital gyrus for left TLE, and increases in betweenness centrality (BC) of bilateral hippocampi for right TLE. A borderline increase in left amygdala betweenness centrality with longer epilepsy duration was also observed in left TLE patients (Table 4).

3. Discussion

We found evidence of reduced functional connectivity (FC) and structural connectivity (SC) in TLE. Functional connectivity was decoupled from structural connectivity in TLE, which lessened with longer epilepsy duration, primarily due to further reduction in functional connectivity. SC–FC decoupling in TLE was identified as mainly attributable to structural and functional changes in the hippocampus, frontal inferior orbital gyrus, and posterior cingulate. Regions contributing to SC–FC decoupling followed a more extensive pattern of structural and functional changes in left TLE, whereas SC–FC decoupling in right TLE involved predominantly bilateral hippocampal functional changes. The increase in SC–FC coupling with longer epilepsy duration was primarily mediated by fusiform and frontal inferior orbital gyrus structural loss for left TLE patients, and by functional increases in hippocampal betweenness centrality in right TLE patients.

3.1. SC–FC coupling in TLE compared to controls

SC–FC decoupling in TLE may be caused by various factors. Whereas a dominant decrease in DTI connectivity suggests white abnormality, a dominant decrease in fMRI connectivity suggests functional abnormalities, such as dysfunctional network nodes or alterations in neurotransmitter levels (Skudlarski et al., 2008). Impaired structural and functional connectivity have been observed consistently in TLE using various imaging methods, including MRI, fMRI, and DTI (Bernhardt et al., 2009; Chiang et al., 2014; Frings et al., 2009; Haneef et al., 2012; Liao et al., 2011). We found that both mean SC and FC of the limbic network were impaired in left TLE, whereas right TLE involved primarily impaired FC. This suggests that left TLE may involve patterns of both white matter as well as functional abnormalities, whereas right TLE may have a more predominant pattern of functional more than white matter abnormalities. Assessment of regional changes indicated that overall, however, the magnitude of impairment was greater for functional than structural connections in both left and right TLE, including major involvement of posterior cingulate

connections to the thalamus, parahippocampal gyrus, and hippocampus. Impaired functional connectivity of the hippocampus, parahippocampus, and thalamus is consistent with previous research, which has also found evidence of reduced fMRI connectivity between the posterior cingulate and hippocampus, as well as decreased functional connectivity of the parahippocampus (James et al., 2013). Thalamic atrophy has also been shown based on cortical thickness measurements (Bernhardt et al., 2012), in addition to gray matter loss in the anterior thalamic nuclei using voxel-based MRI morphometry (Bonilha et al., 2005). Given the projection of the anterior thalamic nuclei to the cingulate gyrus, this is consistent with our finding of decreased functional connectivity between the thalamus and posterior cingulate in TLE. Previous research has found that the thalamus and hippocampus functionally co-activate and are nodes within the same network, suggesting that thalamic damage in TLE may result from network excitotoxicity (Barron et al., 2012).

Since epileptic seizures result from abnormal neuronal excitation and hypersynchronization, the question of why our study and others have observed decreases in mean levels of functional connectivity is interesting. Increasing reports of hub redistribution in TLE (Chiang et al., 2014; Liao et al., 2010; Wilke et al., 2011) suggest that abnormal reinforcement of functional connections through epileptic propagation may lead to the reduction of other normal functional connections which become less used. The increase in functional connectivity between neighbors of the posterior cingulate (increased clustering coefficient (CC) and local efficiency (LE)) observed here, concurrent with decreased pairwise functional connections between the posterior cingulate with the thalamus and hippocampus, also supports the hypothesis that epileptogenically reinforced connections may occur at the expense of others.

3.2. Correlation of SC–FC coupling with TLE duration

An increase in SC–FC coupling was identified with longer TLE duration independent of age. Although an increase in SC–FC coupling with age was also identified here, as it has been identified in previous studies (Hagmann et al., 2010; Supekar et al., 2010), our results show that both age and epilepsy duration exhibit modulatory effects on the level of SC–FC coupling in TLE patients. Presumably, lessening of the dissociation between structural and functional connectivity in TLE may reflect either a compensatory process in which structural–functional coupling increases elsewhere in the network to compensate for the decoupling caused by functional connectivity loss, or regional losses in structural connectivity which balance the decreases in functional connectivity. In either case, both structural and functional TLE networks have demonstrated decreased small-world properties with longer TLE duration, leading to a less optimal structural and functional configurations in patients with longer history of TLE (Bernhardt et al., 2011; van Dellen et al., 2009). Therefore, while SC–FC coupling levels may increase over time in TLE patients, previous research suggests that recovery of an efficient network configuration does not occur.

Despite the fact that SC–FC coupling increased with longer TLE duration, correlations between epilepsy duration and network structural and functional connectivity based on single imaging modalities were not statistically significant. This suggests that SC–FC coupling may provide a more sensitive metric for capturing progressive network changes

with epilepsy duration in TLE, consistent with similar prior observations in idiopathic generalized epilepsy (Zhang et al., 2011). The increased sensitivity of SC–FC coupling to effects from epilepsy duration may be due to its ability, as an integrative measure, to capitalize on the different sensitivities of fMRI and DTI. For example, fMRI has weaker sensitivity in certain portions of the brain, such as near the thalamus, where noise from cardiac and respiratory pulsations is more prominent (Skudlarski et al., 2008). In contrast, DTI tractography has weaker sensitivity in areas of the brain with prolate or isotropic tensors, as well as areas with crossing or kissing fibers (Shetty et al., 2014). By combining data from fMRI and DTI, SC–FC coupling is able to capture durational effects on fMRI connectivity in regions of the brain with low DTI sensitivity, while capturing durational effects on DTI connectivity in regions with low fMRI sensitivity.

3.3. Lateralized differences in SC–FC coupling between left and right TLE

Our observation of decreased limbic structural connectivity in left, but not right, TLE is consistent with other DTI studies of TLE. Using probabilistic tractography, decreases in structural connectivity were found to be more severe in left compared to right TLE (Besson et al., 2014; Kemmotsu et al., 2011). A greater amount of atrophy in left TLE patients has also been identified using voxel-based morphometry (Bonilha et al., 2007) and cortical thickness analyses (Kemmotsu et al., 2011). These results may be an indication of the commonly observed clinical finding of greater cognitive deficits in left TLE (Bonilha et al., 2007; Mayeux et al., 1980) and may potentially reflect greater vulnerability of the left temporal lobe to injury and progressive seizure-induced damage (Kemmotsu et al., 2011; Mullaart et al., 1995). Contribution of anterior cingulate abnormalities to SC–FC decoupling in left but not right TLE may help explain the greater impairment of executive dysfunction in left than right TLE (Strauss et al., 1993), as the anterior cingulate is thought to be involved in higher executive functions (Carter et al., 1999).

On a whole-network level, we found that that SC–FC decoupling occurred to a greater magnitude in left than right TLE patients. Additionally, we found that SC–FC decoupling was mediated by changes in multiple focal regions in left TLE (right fusiform, left frontal inferior orbital gyrus, bilateral posterior cingulate, left anterior cingulate, left caudate), compared to a bilateral pattern of hippocampal abnormality in right TLE. Our finding of a more lateralized decoupling pattern in left TLE is consistent with previous research, which has found that both DTI (Khan et al., 2014) and fMRI (Dupont et al., 2002; Vlooswijk et al., 2010) changes are more lateralized in left TLE. The posterior cingulate gyrus appeared to play a major role in SC– FC decoupling, involving abnormalities in multiple functional topological properties (BC, LE, CC). One caveat is the slightly longer epilepsy duration of our right TLE versus left TLE group, so that epilepsy duration must be considered for its possible effect on these lateralized differences. However, in support of our findings, a previous study has also found that SC–FC decoupling occurs in left but not right TLE patients in language related tracts (Rodrigo et al., 2008). Prior research in which left and right TLE groups were more closely matched on epilepsy duration also identified evidence of posterior cingulate and hippocampal involvement in TLE, with the posterior cingulate found to be more involved in left TLE (James et al., 2013) and bilateral patterns of hippocampal involvement more involved in right TLE (Besson et al., 2014). Evidence of

hippocampal and insula involvement in right TLE compared to posterior cingulate involvement in left TLE has also been confirmed previously by us, as well as the finding that hippocampal changes in between-ness centrality are stronger in right TLE (Chiang et al., 2014). Extensive involvement of posterior cingulate functional changes and hippocampal structural and functional changes is also in line with previous research implicating decreases in both structural and functional connectivity between the posterior cingulate/precuneus and bilateral mesial temporal lobes in TLE (Liao et al., 2011).

3.4. SC-FC coupling in left TLE

The role of the posterior cingulate gyrus in SC-FC decoupling was greater in left than right TLE, including ipsilaterally increased CC, contralaterally decreased BC, and bilaterally increased LE. CC is a measure of cliquishness, or the extent to which a region's neighbors are connected amongst themselves. Therefore, the increase in ipsilateral posterior cingulate CC suggests an ipsilateral increase in local functional connections between neighbors of the posterior cingulate. As the posterior cingulate provides afferent inputs to the hippocampus through the entorhinal cortex, an increase in local functional connectivity between neighbors of the posterior cingulate may presumably involve the hippocampal network. This may reflect the development of recurrent excitatory circuits in the hippocampal network, as well as hippocampal mossy fiber sprouting and synaptic reorganization, which has been observed ipsilaterally in TLE (Mathern et al., 1995; Sutula et al., 1989). This hypothesis is also supported by increased hippocampal-limbic connectivity, which has been observed using seed-based fMRI analysis (Haneef et al., 2014). LE is a related measure to CC and estimates the inverse of the average shortest path length between the neighbors of a given node. The bilateral increase in LE and ipsilateral increase in CC suggest that, while the formation of recurrent circuits may be more dominant ipsilaterally (affecting both CC and LE), the neighbors of the posterior cingulate also become more interconnected contralaterally, inducing changes in LE. BC provides a measure of a node's importance to the network ("hubness"), with high BC indicating nodes that lie on highly traveled paths (Chiang and Haneef, 2014). Our finding of reduced contralateral BC of the posterior cingulate gyrus in left TLE is consistent with the decrease in FC between the posterior cingulate and mesial temporal lobes observed in prior research (Liao et al., 2011). Redistribution of functional hubs in TLE has also been noted in several other studies (Chiang et al., 2014; Liao et al., 2010; Wilke et al., 2011).

Progressive structural loss of the contralateral fusiform and ipsilateral frontal inferior orbital gyrus exhibited significant influences on the increase of SC-FC with longer TLE history, involving decreases in FA and increases in MD. As increased MD generally reflects pathological processes such as necrosis, edema, or inflammation (Alexander et al., 2007), the decrease in FA and increase in MD with longer left TLE duration most likely reflects atrophy of these structures over the disease course. Morphometric research also supports atrophy of the fusiform and frontal inferior orbital gyrus with greater TLE disease burden, finding significant gray matter loss in the fusiform and medial orbital gyrus in patients with greater hippocampal volume loss (Duzel et al., 2006). Cortical thinning in the frontal inferior orbital gyrus of TLE patients (McDonald et al., 2008), as well as decreased cerebral blood flow to the fusiform gyrus in left TLE using PET (Henry et al., 1998), have also been

observed and may follow or contribute to atrophy. Loss of limbic structural integrity may lead to an increase in limbic network coupling levels, by balancing the prominent decreases in functional connectivity present in TLE.

Although these structures experienced a loss of structural integrity with longer epilepsy duration, the limbic network overall experienced no net change in structural connectivity over the TLE disease course. This suggests that progressive structural loss of the fusiform and frontal inferior orbital gyri induces compensatory increases in structural connectivity elsewhere in the network. Future, larger powered studies may be helpful to detect these increases.

3.5. SC–FC coupling in right TLE

Among right TLE patients, functional hippocampal changes were the primary contributors to increased SC–FC coupling with longer epilepsy duration. Bilateral hippocampal changes contributed to the increase in SC–FC coupling, involving progressive increases in BC and marginally significant decreases in CC. Our findings for right TLE patients are concordant with previous research, with previous studies similarly observing bilateral patterns of functional impairment in right TLE (Billingsley et al., 2001; Dupont et al., 2002; Vlooswijk et al., 2010). We also observed a decrease in insula BC concurrent with an increase in bilateral hippocampal BC, which may reflect the redistribution of functional hubs previously reported in TLE (Chiang et al., 2014; Liao et al., 2010; Wilke et al., 2011). The increase in hippocampal betweenness centrality may contribute to increased coupling levels by offsetting pairwise decreases in functional connectivity, such as between the hippocampus and posterior cingulate.

A few aspects of study design should be considered in the interpretation of the present results. As we included only direct functional connections in the construction of our FC network, the results are only relevant to the coupling of first-order functional and structural connectivity. Another consideration is that deterministic tractography fails to account for situations with prolate or isotropic tensors. Tracking may also lead to inference of erroneous directions in the case of crossing or kissing fibers, due to the assumption of a single dominant fiber orientation per voxel (Shetty et al., 2014). Alternative approaches, such as probabilistic or multitensor tractography, may be helpful in future work. However, for the construction of weighted structural networks as employed in this study, deterministic tractography is preferred by estimating connection strengths rather than probabilities (Schmidt et al., 2014). Another consideration is that the fMRI repetition time utilized in this study was 6000 ms. Although a bandpass filter of 0.01–0.08 Hz was applied in order to sample low-frequency fluctuations in this range, the sensitivity of correlation maps produced by lower sampling rates may be decreased, due to the aliasing of physiological noise such as cardiac or respiratory pulsations into the evaluated passband. Another limitation of this study is the moderate sample size (N=34), which yields less power for detecting associations. The associations reported in this study are likely to be among the stronger associations which may exist, and warrant confirmation through larger sample studies. The cross-sectional design of this study for assessing the effects of TLE progression on SC–FC coupling is also not ideal due to potential confounding effects of age, due to the high correlation of age with

TLE duration. Although we corrected for age in correlational assessments, the decreased effect size may have also hindered detection of more subtle progressive changes. Caution is also advisable in interpreting results due to the difference in epilepsy duration between left and right TLE patients. Although not significant, our left TLE study sample had a lower mean epilepsy duration than the right TLE group, which may provide an explanation for why SC–FC coupling was not as severely decreased in right as in left TLE. This corresponded with a significantly older mean age of epilepsy onset for the left TLE study sample (p=0.02; Mann-Whitney U test). Heterogeneity in age of onset may lead to differences in functional connectivity (Doucet et al., 2015) and may also have an impact on SC–FC coupling. However, the lateralized differences reported in our study are largely supported by evidence from previous research. Future, larger studies employing matched left and right TLE groups are needed to confirm the lateralized differences explored in our study. Future studies in which patients are matched on the individual subject level rather than on the group level may also be advantageous to validating the results of this study.

In summary, functional connectivity was decoupled from structural connectivity in TLE, with an increase in coupling occurring with longer duration of TLE. SC–FC coupling was mediated by regional changes most prominently in the fusiform gyrus, frontal inferior orbital gyrus, and posterior cingulate in left TLE, and in the hippocampus in right TLE. Improved understanding of the relationship between structural and functional connectivity in TLE may provide better biomarkers through insight obtained by integrating imaging modalities.

4. Disclosure statement

1. Dr Engel has patents WO 2009/123734A1, and WO 2009/ 123735A1, receives royalties from MedLink, Wolters Kluwer, Blackwell, and Elsevier, and has received honoraria from Medtronics, Wolters Kluwer, and Best Doctors.
2. Dr. Stern has served as a paid consultant for UCB, Lundbeck and Sunovion. Dr. Stern is an editor of MedLink Neurology, and has received royalties from Wolters Kluwer and from McGraw-Hill.
3. The remaining authors have no disclosures/ conflicts of interest.

5. Experimental procedure

5.1. Subjects

The study population was composed of 24 TLE patients (14 left TLE, 10 right TLE) and 11 healthy controls. Control subjects were recruited through university advertisement and word-of-mouth, and none had a history of neurological illness or were taking neurological medications. TLE patients were recruited from the BCM comprehensive epilepsy center following clinical evaluation, video-EEG monitoring, and high-resolution MRI. Patients with disabling cognitive impairment or other neurological comorbidities were excluded. Written informed consent was obtained prior to scanning for all subjects. The study was approved by the Baylor College of Medicine (BCM) Institutional Review Board.

5.2. Image acquisition

Imaging was performed on a Philips Ingenia 3.0 T MRI scanner (Philips Medical Systems, Best, Netherlands) equipped with a 16 channel digital RF coil for signal reception. Resting state fMRI was acquired axially for 10min (TR=6000 ms, TE=30ms, FOV=228mm, matrix=100 × 100, slice thickness=2.25 mm, 67 slices, 100 volumes). Subjects were instructed to lie still with eyes closed, and not asked to think about anything in particular during the functional sequence. Patients were requested not to fall asleep during imaging and were monitored by the imaging technician. T1-weighted imaging was also performed as follows: TR=2500ms, TE=4600ms, FOV=199mm, matrix = 244 × 206, slice thickness=1.4 mm, 284 slices. A SE-EPI based DTI sequence was acquired with the following acquisition parameters: FOV=228 mm × 228 mm × 143 mm, acquired voxel size=2 mm × 2 mm × 2.2 mm (i.e., 65 slices at 2.2 mm thick), TR/ TE=9400ms/75ms, parallel imaging acceleration factor=2.5, b-values acquired: 0 (3 NSA) and 1000 (1 NSA along 32 directions) s/mm^2, chemical shift selective fat suppression. Slices were acquired in axial-oblique orientation.

5.3. fMRI processing and functional network construction

fMRI preprocessing was performed using FSL (fMRIB Software Library) version 5.0.2 (Oxford, UK, www.fmrib.ox.ac.uk/fsl). The first 12 s were discarded to attain magnetization equilibrium. Resting state functional images underwent included non-brain tissue elimination (Smith, 2002), slice-timing correction, spatial smoothing using a Gaussian kernel (5 mm full-width half maximum), linear co-registration to the T1-weighted image, temporal bandpass filtering (0.01 <f < 0.08 Hz consistent with TR 6000 ms) (Fox et al., 2005; Uddin et al., 2009), motion scrubbing through nuisance regression (Power et al., 2012), and removal of various sources of spurious variance using linear regression including six motion parameters and their temporal derivatives, and ventricular and white matter signal (Fox et al., 2005). Residuals were normalized prior to analysis.

After linear registration to the Montreal Neurological Institute (MNI) standard template, functional images were parcellated into 90 cortical and subcortical regions defined by the automated anatomical labeling (AAL) atlas (Tzourio-Mazoyer et al., 2002). For each subject, FC was estimated between ten pairs of bilateral limbic and peri-limbic structures previously implicated in TLE (Fig. 1) (Bonilha et al., 2012), based on the Pearson correlation between BOLD residual time series averaged across all voxels in each region.

5.4. DTI processing and structural network construction

Diffusion gradient directions were extracted using CATNAP (Landman et al., 2013). For each subject, non-diffusion weighted b0 images (b=0 s/mm^2) and T1-weighted images underwent non-brain tissue elimination. Diffusion-weighted images were eddy-current corrected and co-registered to the b0 image in order to minimize head movement using FSL. Diffusion tensors were estimated using the TrackVis Diffusion Toolkit (Wang et al., 2007), and whole-brain deterministic tractography performed in native diffusion space using the FACT algorithm (Mori and van Zijl, 2002). Tractography was terminated if it reached a fractional anisotropy threshold of < 0.2 or a primary eigenvector turning angle of >35 degrees (Mori et al., 2002).

To obtain each subject's SC matrix, each subject's brain was parcellated in native diffusion space using the same nodes as in functional network to allow for comparability. Each structural T1-weighted image was first linearly co-registered to the b0 image and transformed to the ICBM-152 MNI T1 template. Inverse deformation maps were applied to AAL regions to warp regions to native diffusion space (Gong et al., 2009; Li et al., 2009; Zhang et al., 2011). Using the UCLA Multimodal Connectivity Package, two regions were considered structurally connected if at least three fibers had one endpoint which terminated in one region and another which terminated in the other region (Shu et al., 2009, 2011). This threshold was used in order to decrease the risk of false positive edges. Fiber densities were then mapped to connection strengths following previous work (Hagmann et al., 2008; Honey et al., 2009; van den Heuvel et al., 2013), in which nonzero fiber densities were resampled to a Gaussian distribution with mean 0.5 and standard deviation of 0.1 (Honey et al., 2009; van den Heuvel et al., 2013).

5.5. Structural–functional coupling

For each subject, a structural–functional (SC–FC) coupling metric was estimated as the Spearman correlation between structural and functional connection strengths (Honey et al., 2009; van den Heuvel et al., 2013). We used the Spearman correlation coefficient as a measure of monotonic statistical dependency, in order to capture both linear and nonlinear associations between structural and functional connectivity. In particular, for each subject, the Spearman correlation was computed between the pairwise SC strengths between regions j and k, $(SC_{jk}\}_{j\neq k}$ and the pairwise FC strengths between regions j and k, $(FC_{jk})_{j\neq k}$. Computation of SC–FC coupling from each subject's fMRI and DTI scan is summarized in Fig. 2.

5.6. Groupwise comparison

Non-parametric permutation testing based on 10,000 resamples was used to compare SC–FC coupling, mean network SC, and mean network FC between left/right TLE patients and healthy controls. Outliers located outside 1.5 times the interquartile range above/below the upper/lower quartiles were excluded. Regional differences in pairwise SC and pairwise FC strengths were also compared between left/right TLE patients and controls using permutation testing based on 10,000 resamples. Significance was evaluated after multiple testing correction by controlling the false discovery rate (FDR) at the 0.05 level (Benjamini and Hochberg, 1995).

5.7. Correlation of SC–FC coupling with epilepsy duration

The association of SC–FC coupling with epilepsy duration was evaluated using the Pearson correlation coefficient (r). Influential observations with a Cook's distance > 1 were removed. In order to adjust estimated correlations for potential confounding effects of age and gender, the change-in-estimate (CE) criterion was used, with covariates identified as confounders if the Pearson correlation changed by more than 10% when the covariate was added to the model. The CE criterion was chosen as it is less influenced by sample size than use of significance testing criteria for confounder identification (Tong and Lu, 2001). The partial Pearson correlation controlling for identified con-founders was then used to evaluate the relationship between SC–FC coupling and epilepsy duration.

To identify whether the correlation of SC–FC coupling with epilepsy duration is more affected by SC or FC changes, we used the semi-partial Pearson correlation to estimate the effect on SC–FC progression when mean structural (or functional) connectivity was held constant. Larger CE values (CE_{SC} or CE_{FC}) indicated a greater relative impact on progression of SC–FC coupling. Directionality of progressive changes in SC and FC was evaluated using the Pearson correlation coefficient.

5.8. Regional structural and functional factors in SC–FC coupling

To identify which structural and functional regional changes are responsible for SC–FC decoupling in TLE in a multivariate context, we next computed regional functional graph theory metrics (betweenness centrality, BC; local efficiency, LE; clustering coefficient, CC) as well as measures of structural integrity (fractional anisotropy, FA; mean diffusivity, MD) for each of the 20 limbic/peri-limbic regions of interest (Appendix A). Elastic net (EN) regression was used to identify associations between SC–FC coupling and regional structural/functional changes, in order to account for multicollinearity and the greater number of predictor variables than observations. EN uses a linear combination of L1 and L2 penalties in estimating regression coefficients, in order to produce a sparse solution via the L1 penalty while encouraging a grouping effect and stabilizing the L1 regularization path via the L2 penalty. This has been shown to be especially useful in collinear data with $n \ll p$ (Zou and Hastie, 2005). We set the weight of the L1 penalty $\alpha = 0.5$ and the regularization parameter λ chosen by 5-fold cross-validation to minimize cross-validation error. The optimal λ value was used for variable selection. Variables were standardized by centering and scaling prior to analysis. To increase robustness of the cross-validation procedure to fold variance, multiple repeat cross-validation was used. Specifically, the cross-validated EN procedure was repeated 1000 times (Kohavi, 1995), in order to generate a ranked list of variables based on variable inclusion probability (VIP), computed as the frequency of selection among all cross-validation runs. The same procedure was also applied to individual left TLE and right TLE subgroups, in order to identify lateralized differences in regional factors. Features were considered associated with the dependent variable if selected in > 50% of EN cross-validation runs, and are listed in Table 2 and Table 3 in order of decreasing VIP. A conservative threshold of 50% was chosen in order to avoid missing relevant predictors (Bunea et al., 2011).

5.9. Regional mediators of progressive increase in SC–FC coupling

Lastly, we evaluated which structural and functional regional changes mediate the increase in SC–FC coupling with longer epilepsy duration. Variables were identified as significant third-party mediators of the increase in SC–FC coupling with epilepsy duration if, in addition to a significant association between epilepsy duration and SC–FC coupling, the mediator was significantly correlated with the exposure (epilepsy duration) at the 0.05 level as well as VIP > 0.50 with the outcome of interest (SC–FC coupling) (Baron and Kenny, 1986; Bauman et al., 2002). Correlation with epilepsy duration was estimated based on the Pearson correlation coefficient.

Supplementary Material

Refer to Web version on PubMed Central for supplementary material.

Acknowledgments

Funding/ support for this research was provided by (1) the National Library of Medicine Training Fellowship in Biomedical Informatics, Gulf Coast Consortia for Quantitative Bio-medical Sciences (Grant #2T15LM007093-21) (SC); (2) the National Institute of Health (Grant #5T32CA096520-07) (SC); (3) NIH-NINDS K23 Grant NS044936 (JMS); (4) The Leff Family Foundation (JMS); (5) NIH Grants P01 NS02808, R01 NS33310, and U01 NS42372 (JE); (6) The Epilepsy Foundation of America (award ID 244976) (ZH); (7) Baylor College of Medicine Computational and Integrative Biomedical Research Center (CIBR) Seed Grant Awards (ZH); (8) Baylor College of Medicine Junior Faculty Seed Funding Program Grant (ZH).

Abbreviations

SC	structural connectivity
FC	functional connectivity
TLE	temporal lobe epilepsy
DTI	diffusion tensor imaging
EN	elastic net
FA	fractional anisotropy
MD	mean diffusivity
BC	betweenness centrality
LE	local efficiency
CC	clustering coefficient
MNI	Montreal Neurological Institute
AAL	automated anatomical labeling
FDR	false discovery rate
CE	change-in-estimate
VIP	variable importance measure

REFERENCE

Alexander AL, Lee JE, Lazar M, Field AS. Diffusion tensor imaging of the brain. Neurotherapeutics. 2007; 4:316–329. [PubMed: 17599699]

Avoli M, D'Antuono M, Louvel J, Kohling R, Biagini G, Pumain R, D'Arcangelo G, Tancredi V. Network and pharmacological mechanisms leading to epileptiform synchronization in the limbic system in vitro. Prog. Neurobiol. 2002; 68:167–207. [PubMed: 12450487]

Baron RM, Kenny DA. The moderator-mediator variable distinction in social psychological research: conceptual, strategic, and statistical considerations. J. Pers. Soc. Psychol. 1986; 51:1173–1182. [PubMed: 3806354]

Barron DS, Fox PM, Laird AR, Robinson JL, Fox PT. Thalamic medial dorsal nucleus atrophy in medial temporal lobe epilepsy: a VBM meta-analysis. NeuroImage Clin. 2012; 2:25–32. [PubMed: 24179755]

Bauman AE, Sallis JF, Dzewaltowski DA, Owen N. Toward a better understanding of the influences on physical activity: the role of determinants, correlates, causal variables, mediators, moderators, and confounders. Am. J. Prev. Med. 2002; 23:5–14. [PubMed: 12133733]

Benjamini Y, Hochberg Y. Controlling the false discovery rate: a practical and powerful approach to multiple testing. J. R. Stat. Soc. Ser. B (Methodological). 1995:289–300.

Bernhardt BC, Bernasconi N, Kim H, Bernasconi A. Mapping thalamocortical network pathology in temporal lobe epilepsy. Neurology. 2012; 78:129–136. [PubMed: 22205759]

Bernhardt BC, Chen Z, He Y, Evans AC, Bernasconi N. Graph-theoretical analysis reveals disrupted small-world organization of cortical thickness correlation networks in temporal lobe epilepsy. Cereb. Cortex. 2011; 21:2147–2157. [PubMed: 21330467]

Bernhardt BC, Worsley KJ, Kim H, Evans AC, Bernasconi A, Bernasconi N. Longitudinal and cross-sectional analysis of atrophy in pharmacoresistant temporal lobe epilepsy. Neurology. 2009; 72:1747–1754. [PubMed: 19246420]

Bertram EH, Zhang DX, Mangan P, Fountain N, Rempe D. Functional anatomy of limbic epilepsy: a proposal for central synchronization of a diffusely hyperexcitable network. Epilepsy Res. 1998; 32:194–205. [PubMed: 9761320]

Besson P, Dinkelacker V, Valabregue R, Thivard L, Leclerc X, Baulac M, Sammler D, Colliot O, Lehericy S, Samson S, Dupont S. Structural connectivity differences in left and right temporal lobe epilepsy. NeuroImage. 2014; 100:135–144. [PubMed: 24814212]

Billingsley RL, McAndrews MP, Crawley AP, Mikulis DJ. Functional MRI of phonological and semantic processing in temporal lobe epilepsy. Brain. 2001; 124:1218–1227. [PubMed: 11353737]

Bonilha L, Alessio A, Rorden C, Baylis G, Damasceno BP, Min LL, Cendes F. Extrahippocampal gray matter atrophy and memory impairment in patients with medial temporal lobe epilepsy. Hum. Brain Mapp. 2007; 28:1376–1390. [PubMed: 17370345]

Bonilha L, Nesland T, Martz GU, Joseph JE, Spampinato MV, Edwards JC, Tabesh A. Medial temporal lobe epilepsy is associated with neuronal fibre loss and paradoxical increase in structural connectivity of limbic structures. J. Neurol. Neurosurg. Psychiatry. 2012; 83:903–909. [PubMed: 22764263]

Bonilha L, Rorden C, Castellano G, Cendes F, Li LM. Voxel-based morphometry of the thalamus in patients with refractory medial temporal lobe epilepsy. NeuroImage. 2005; 25:1016–1021. [PubMed: 15809001]

Bunea F, She Y, Ombao H, Gongvatana A, Devlin K, Cohen R. Penalized least squares regression methods and applications to neuroimaging. NeuroImage. 2011; 55:1519–1527. [PubMed: 21167288]

Carter CS, Botvinick MM, Cohen JD. The contribution of the anterior cingulate cortex to executive processes in cognition. Rev. Neurosci. 1999; 10:49–58. [PubMed: 10356991]

Chiang S, Haneef Z. Graph theory findings in the pathophysiology of temporal lobe epilepsy. Clin. Neurophysiol. 2014; 125:1295–1305. [PubMed: 24831083]

Chiang S, Stern JM, Engel J Jr, Levin HS, Haneef Z. Differences in graph theory functional connectivity in left and right temporal lobe epilepsy. Epilepsy Res. 2014; 108:1770–1781. [PubMed: 25445238]

Concha L, Beaulieu C, Gross DW. Bilateral limbic diffusion abnormalities in unilateral temporal lobe epilepsy. Ann. Neurol. 2005; 57:188–196. [PubMed: 15562425]

Deco G, Jirsa VK, McIntosh AR. Emerging concepts for the dynamical organization of resting-state activity in the brain. Nat. Rev. Neurosci. 2011; 12:43–56. [PubMed: 21170073]

Doucet GE, Sharan A, Pustina D, Skidmore C, Sperling MR, Tracy JI. Early and late age of seizure onset have a differential impact on brain resting-state organization in temporal lobe epilepsy. Brain Topogr. 2015; 28:113–126. [PubMed: 24881003]

Dupont S, Samson Y, Van de Moortele PF, Samson S, Poline JB, Hasboun D, Le Bihan D, Baulac M. Bilateral hemispheric alteration of memory processes in right medial temporal lobe epilepsy. J. Neurol. Neurosurg. Psychiatry. 2002; 73:478–485. [PubMed: 12397138]

Duzel E, Schiltz K, Solbach T, Peschel T, Baldeweg T, Kaufmann J, Szentkuti A, Heinze HJ. Hippocampal atrophy in temporal lobe epilepsy is correlated with limbic systems atrophy. J. Neurol. 2006; 253:294–300. [PubMed: 16133718]

Engel J Jr, Thompson PM, Stern JM, Staba RJ, Bragin A, Mody I. Connectomics and epilepsy. Curr. Opin. Neurol. 2013; 26:186–194. [PubMed: 23406911]

Fox MD, Snyder AZ, Vincent JL, Corbetta M, Van Essen DC, Raichle ME. The human brain is intrinsically organized into dynamic, anticorrelated functional networks. Proc. Natl. Acad. Sci. U.S.A. 2005; 102:9673–9678. [PubMed: 15976020]

Frings L, Schulze-Bonhage A, Spreer J, Wagner K. Remote effects of hippocampal damage on default network connectivity in the human brain. J. Neurol. 2009; 256:2021–2029. [PubMed: 19603243]

Gong G, He Y, Concha L, Lebel C, Gross DW, Evans AC, Beaulieu C. Mapping anatomical connectivity patterns of human cerebral cortex using in vivo diffusion tensor imaging tractography. Cereb. Cortex. 2009; 19:524–536. [PubMed: 18567609]

Greicius MD, Supekar K, Menon V, Dougherty RF. Resting-state functional connectivity reflects structural connectivity in the default mode network. Cereb. Cortex. 2009; 19:72–78. [PubMed: 18403396]

Hagmann P, Cammoun L, Gigandet X, Meuli R, Honey CJ, Wedeen VJ, Sporns O. Mapping the structural core of human cerebral cortex. PLoS Biol. 2008; 6:e159. [PubMed: 18597554]

Hagmann P, Sporns O, Madan N, Cammoun L, Pienaar R, Wedeen VJ, Meuli R, Thiran JP, Grant PE. White matter maturation reshapes structural connectivity in the late developing human brain. Proc. Natl. Acad. Sci. U.S.A. 2010; 107:19067–19072. [PubMed: 20956328]

Haneef Z, Lenartowicz A, Yeh HJ, Engel J Jr, Stern JM. Effect of lateralized temporal lobe epilepsy on the default mode network. Epilepsy Behav. 2012; 25:350–357. [PubMed: 23103309]

Haneef Z, Lenartowicz A, Yeh HJ, Levin HS, Engel J Jr, Stern JM. Functional connectivity of hippocampal networks in temporal lobe epilepsy. Epilepsia. 2014; 55:137–145. [PubMed: 24313597]

Henry TR, Buchtel HA, Koeppe RA, Pennell PB, Kluin KJ, Minoshima S. Absence of normal activation of the left anterior fusiform gyrus during naming in left temporal lobe epilepsy. Neurology. 1998; 50:787–790. [PubMed: 9521277]

Honey CJ, Sporns O, Cammoun L, Gigandet X, Thiran JP, Meuli R, Hagmann P. Predicting human resting-state functional connectivity from structural connectivity. Proc. Natl. Acad. Sci. U.S.A. 2009; 106:2035–2040. [PubMed: 19188601]

James GA, Tripathi SP, Ojemann JG, Gross RE, Drane DL. Diminished default mode network recruitment of the hippocampus and parahippocampus in temporal lobe epilepsy. J. Neurosurg. 2013; 119:288–300. [PubMed: 23706058]

Kemmotsu N, Girard HM, Bernhardt BC, Bonilha L, Lin JJ, Tecoma ES, Iragui VJ, Hagler DJ Jr, Halgren E, McDonald CR. MRI analysis in temporal lobe epilepsy: cortical thinning and white matter disruptions are related to side of seizure onset. Epilepsia. 2011; 52:2257–2266. [PubMed: 21972957]

Khan AR, Goubran M, de Ribaupierre S, Hammond RR, Burneo JG, Parrent AG, Peters TM. Quantitative relaxometry and diffusion MRI for lateralization in MTS and non-MTS temporal lobe epilepsy. Epilepsy Res. 2014; 108:506–516. [PubMed: 24423692]

Kohavi R. A Study of Cross-validation and Bootstrap for Accuracy Estimation and Model Selection. Montreal, Quebec, Canada. 1995:1137–1145.

Landman BA, Bogovic JA, Carass A, Chen M, Roy S, Shiee N, Yang Z, Kishore B, Pham D, Bazin PL, Resnick SM, Prince JL. System for integrated neuroimaging analysis and processing of structure. Neuroinformatics. 2013; 11:91–103. [PubMed: 22932976]

Li Y, Liu Y, Li J, Qin W, Li K, Yu C, Jiang T. Brain anatomical network and intelligence. PLoS Comput. Biol. 2009; 5:e1000395. [PubMed: 19492086]

Liao W, Zhang Z, Pan Z, Mantini D, Ding J, Duan X, Luo C, Lu G, Chen H. Altered functional connectivity and small-world in mesial temporal lobe epilepsy. PLoS One. 2010; 5:e8525. [PubMed: 20072616]

Liao W, Zhang Z, Pan Z, Mantini D, Ding J, Duan X, Luo C, Wang Z, Tan Q, Lu G. Default mode network abnormalities in mesial temporal lobe epilepsy: a study combining fMRI and DTI. Hum. Brain Mapp. 2011; 32:883–895. [PubMed: 20533558]

Mathern GW, Pretorius JK, Babb TL, Quinn B. Unilateral hippocampal mossy fiber sprouting and bilateral asymmetric neuron loss with episodic postictal psychosis. J. Neurosurg. 1995; 82:228–233. [PubMed: 7815150]

Mayeux R, Brandt J, Rosen J, Benson DF. Interictal memory and language impairment in temporal lobe epilepsy. Neurology. 1980; 30:120–125. [PubMed: 7188792]

McDonald CR, Hagler DJ Jr, Ahmadi ME, Tecoma E, Iragui V, Gharapetian L, Dale AM, Halgren E. Regional neocortical thinning in mesial temporal lobe epilepsy. Epilepsia. 2008; 49:794–803. [PubMed: 18266751]

Mori S, Kaufmann WE, Davatzikos C, Stieltjes B, Amodei L, Fredericksen K, Pearlson GD, Melhem ER, Solaiyappan M, Raymond GV, Moser HW, van Zijl PC. Imaging cortical association tracts in the human brain using diffusion-tensor-based axonal tracking. Magn. Reson. Med. 2002; 47:215–223. [PubMed: 11810663]

Mori S, van Zijl P. Fiber tracking: principles and strategies —a technical review. NMR Biomed. 2002; 15:468–480. [PubMed: 12489096]

Mullaart RA, Daniels O, Hopman JC, de Haan AF, Stoelinga GB, Rotteveel JJ. Asymmetry of the cerebral blood flow: an ultrasound Doppler study in preterm newborns. Pediatr. Neurol. 1995; 13:319–322. [PubMed: 8771167]

Power JD, Barnes KA, Snyder AZ, Schlaggar BL, Petersen SE. Spurious but systematic correlations in functional connectivity MRI networks arise from subject motion. NeuroImage. 2012; 59:2142–2154. [PubMed: 22019881]

Rodrigo S, Oppenheim C, Chassoux F, Hodel J, de Vanssay A, Baudoin-Chial S, Devaux B, Meder JF. Language lateralization in temporal lobe epilepsy using functional MRI and probabilistic tractography. Epilepsia. 2008; 49:1367–1376. [PubMed: 18410362]

Schmidt R, Verstraete E, de Reus MA, Veldink JH, van den Berg LH, van den Heuvel MP. Correlation between structural and functional connectivity impairment in amyotrophic lateral sclerosis. Hum. Brain Mapp. 2014; 35:4386–4395. [PubMed: 24604691]

Shetty AN, Chiang S, Maletic-Savatic M, Kasprian G, Vannucci M, Lee W. Spatial mapping of translational diffusion coefficients using diffusion tensor imaging: a mathematical description. Concepts Magn. Reson. Part A. 2014; 43:1–27.

Shu N, Liu Y, Li J, Li Y, Yu C, Jiang T. Altered anatomical network in early blindness revealed by diffusion tensor tractography. PLoS One. 2009; 4:e7228. [PubMed: 19784379]

Shu N, Liu Y, Li K, Duan Y, Wang J, Yu C, Dong H, Ye J, He Y. Diffusion tensor tractography reveals disrupted topological efficiency in white matter structural networks in multiple sclerosis. Cereb. Cortex. 2011; 21:2565–2577. [PubMed: 21467209]

Skudlarski P, Jagannathan K, Calhoun VD, Hampson M, Skudlarska BA, Pearlson G. Measuring brain connectivity: diffusion tensor imaging validates resting state temporal correlations. NeuroImage. 2008; 43:554–561. [PubMed: 18771736]

Smith SM. Fast robust automated brain extraction. Hum. Brain Mapp. 2002; 17:143–155. [PubMed: 12391568]

Strauss E, Hunter M, Wada J. Wisconsin Card Sorting Performance: effects of age of onset of damage and laterality of dysfunction. J. Clin. Exp. Neuropsychol. 1993; 15:896–902. [PubMed: 8120126]

Sun Y, Yin Q, Fang R, Yan X, Wang Y, Bezerianos A, Tang H, Miao F, Sun J. Disrupted functional brain connectivity and its association to structural connectivity in amnestic mild cognitive impairment and Alzheimer's disease. PLoS One. 2014; 9:e96505. [PubMed: 24806295]

Supekar K, Uddin LQ, Prater K, Amin H, Greicius MD, Menon V. Development of functional and structural connectivity within the default mode network in young children. NeuroImage. 2010; 52:290–301. [PubMed: 20385244]

Sutula T, Cascino G, Cavazos J, Parada I, Ramirez L. Mossy fiber synaptic reorganization in the epileptic human temporal lobe. Ann. Neurol. 1989; 26:321–330. [PubMed: 2508534]

Tong IS, Lu Y. Identification of confounders in the assessment of the relationship between lead exposure and child development. Ann. Epidemiol. 2001; 11:38–45. [PubMed: 11164118]

Tzourio-Mazoyer N, Landeau B, Papathanassiou D, Crivello F, Etard O, Delcroix N, Mazoyer B, Joliot M. Automated anatomical labeling of activations in SPM using a macroscopic anatomical parcellation of the MNI MRI single-subject brain. NeuroImage. 2002; 15:273–289. [PubMed: 11771995]

Uddin LQ, Kelly AM, Biswal BB, Castellanos FX, Milham MP. Functional connectivity of default mode network components: correlation, anticorrelation, and causality. Hum. Brain Mapp. 2009; 30:625–637. [PubMed: 18219617]

van Dellen E, Douw L, Baayen JC, Heimans JJ, Ponten SC, Vandertop WP, Velis DN, Stam CJ, Reijneveld JC. Long-term effects of temporal lobe epilepsy on local neural networks: a graph theoretical analysis of corticography recordings. PLoS One. 2009; 4:e8081. [PubMed: 19956634]

van den Heuvel MP, Sporns O, Collin G, Scheewe T, Mandl RC, Cahn W, Goni J, Hulshoff Pol HE, Kahn RS. Abnormal rich club organization and functional brain dynamics in schizophrenia. JAMA Psychiatry. 2013; 70:783–792. [PubMed: 23739835]

van Diessen E, Diederen SJ, Braun KP, Jansen FE, Stam CJ. Functional and structural brain networks in epilepsy: what have we learned? Epilepsia. 2013; 54:1855–1865. [PubMed: 24032627]

Vlooswijk MC, Jansen JF, de Krom MC, Majoie HM, Hofman PA, Backes WH, Aldenkamp AP. Functional MRI in chronic epilepsy: associations with cognitive impairment. Lancet Neurol. 2010; 9:1018–1027. [PubMed: 20708970]

Voets NL, Adcock JE, Stacey R, Hart Y, Carpenter K, Matthews PM, Beckmann CF. Functional and structural changes in the memory network associated with left temporal lobe epilepsy. Hum. Brain Mapp. 2009; 30:4070–4081. [PubMed: 19517529]

Wang R, Benner T, Sorensen A, Wedeen V. Diffusion Toolkit: A Software Package for Diffusion Imaging Data Processing and Tractography. 2007:3720.

Wilke C, Worrell G, He B. Graph analysis of epileptogenic networks in human partial epilepsy. Epilepsia. 2011; 52:84–93. [PubMed: 21126244]

Zhang Z, Liao W, Chen H, Mantini D, Ding JR, Xu Q, Wang Z, Yuan C, Chen G, Jiao Q, Lu G. Altered functional-structural coupling of large-scale brain networks in idiopathic generalized epilepsy. Brain. 2011; 134:2912–2928. [PubMed: 21975588]

Zhu D, Zhang T, Jiang X, Hu X, Chen H, Yang N, Lv J, Han J, Guo L, Liu T. Fusing DTI and fMRI data: a survey of methods and applications. NeuroImage. 2013

Zou H, Hastie T. Regularization and variable selection via the elastic net. J. R. Stat. Soc.: Ser. B (Stat. Methodol). 2005; 67:301–320.

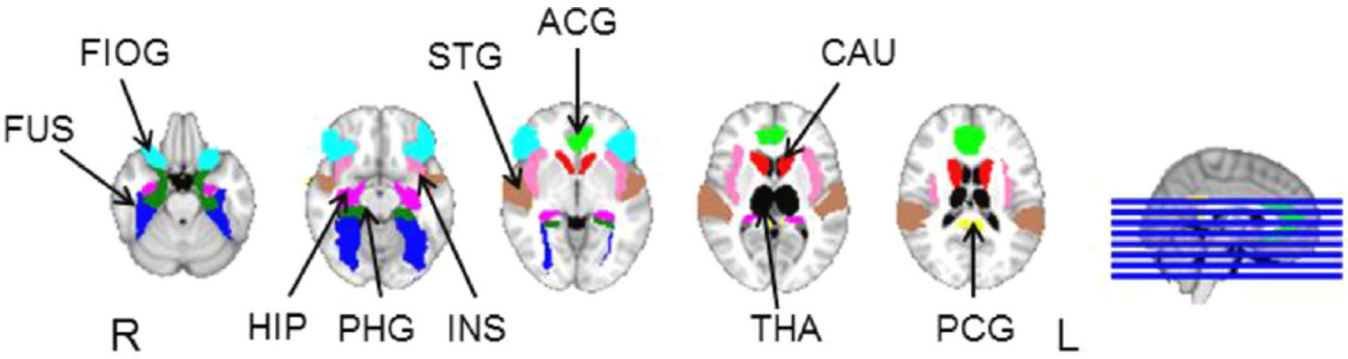

Fig. 1.

Limbic and perilimbic regions of interest examined in this study, overlaid on T1-weighted image in Montreal Neurological Institute standard space. Regions of interest included the anterior cingulate gyrus (ACG), caudate (CAU), fusiform gyrus (FUS), hippocampus (HIP), frontal inferior orbital gyrus (FIOG), insula (INS), parahippocampus (PHG), posterior cingulate gyrus (PCG), superior temporal gyrus (STG), and thalamus (THA). Orientation is radiological. R, right; L, left.

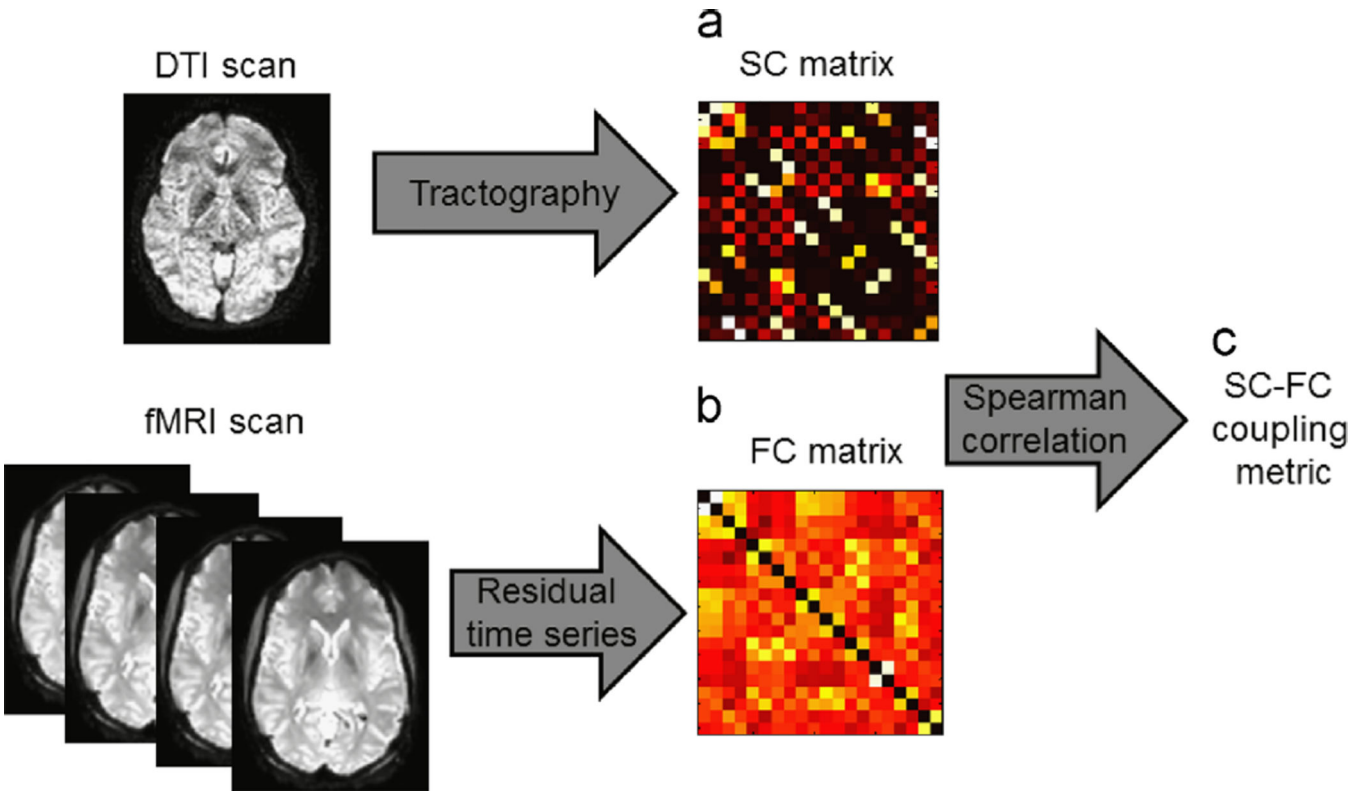

Fig. 2.

Schematic illustrating computation of SC–FC metric from fMRI and diffusion tensor imaging data. (a) Structural connectivity (SC) matrix is computed from DTI using tractography. (b) Functional connectivity (FC) matrix is computed from fMRI using the Pearson correlation between residual time series. (c) SC–FC coupling metric is calculated as the Spearman correlation between SC and FC matrices.

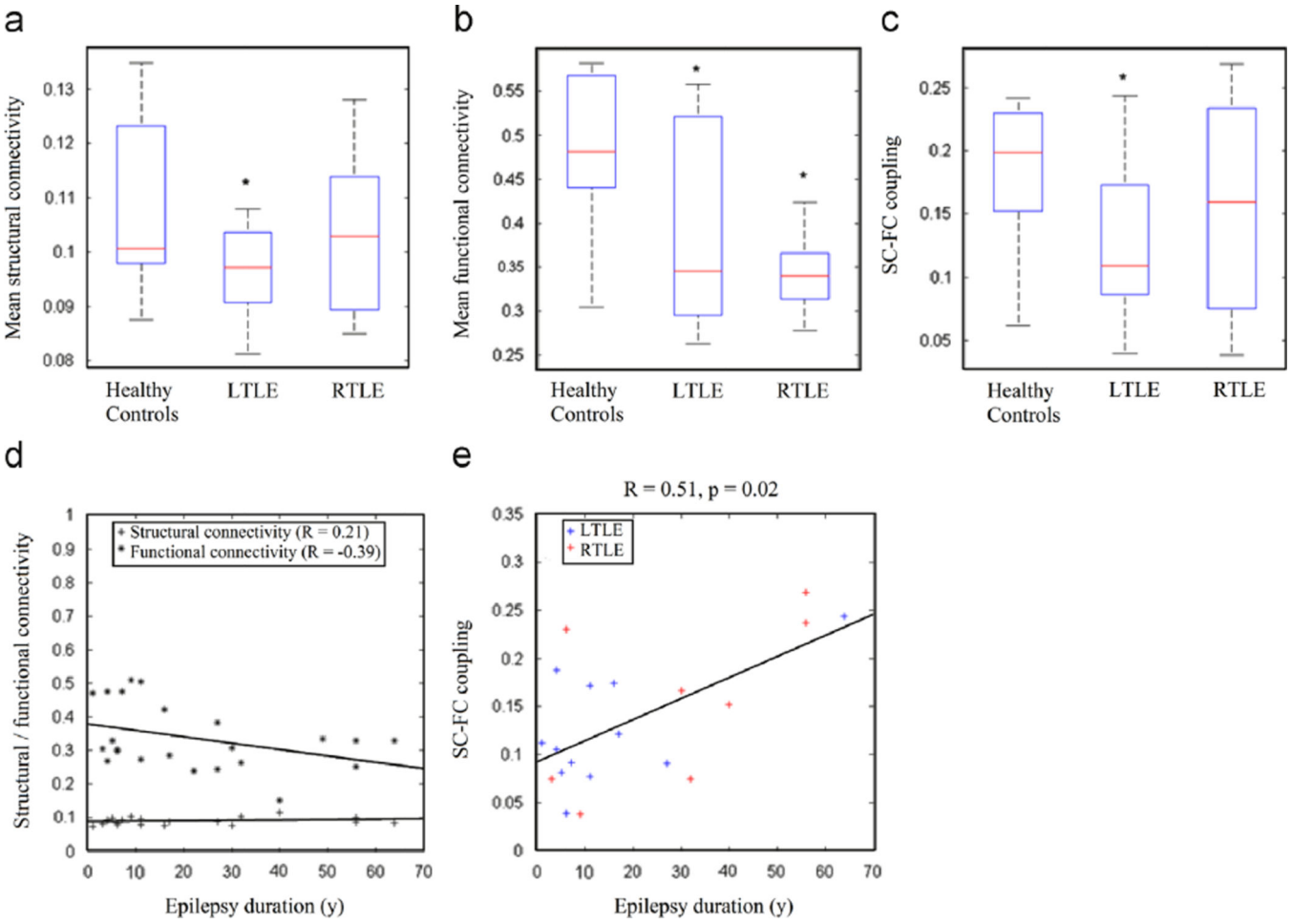

Fig. 3.

Comparison of (a) mean SC, (b) mean FC, and (c) SC–FC coupling for left TLE, right TLE, and healthy controls. Progression of (d) mean SC and FC and (e) SC–FC coupling with epilepsy duration are also shown. SC, structural connectivity; FC, functional connectivity.

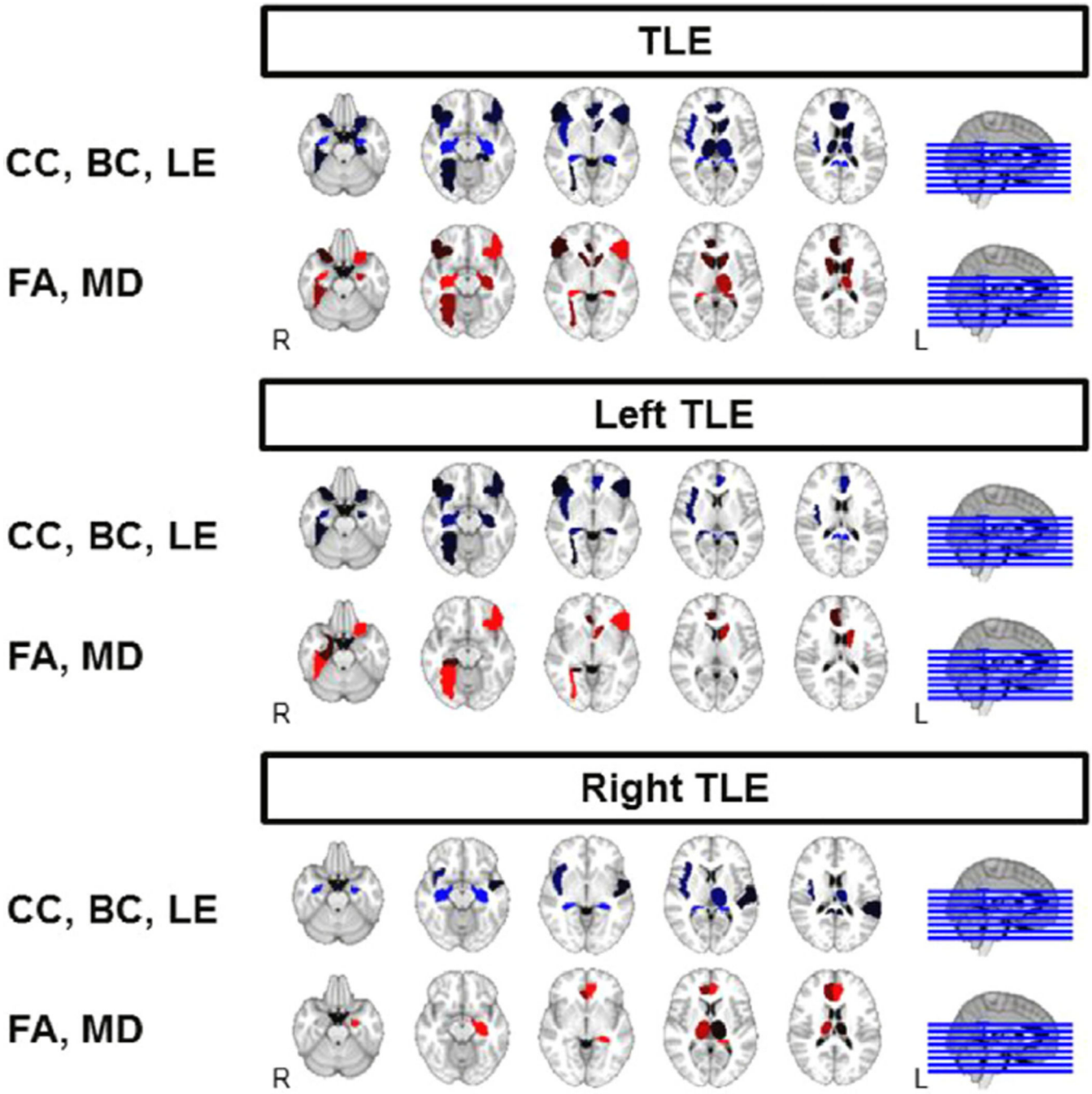

Fig. 4.

Comparison of regional structural and functional measures associated with SC–FC coupling levels in TLE. Brighter color indicates greater magnitude of association with SC–FC coupling. Orientation is radiological. CC, clustering coefficient; LE, local efficiency; BC, betweenness centrality; FA, fractional anisotropy; MD, mean diffusivity; R, right; L, left.

Table 1

Summary demographic details for subject groups.

				p-Value		
	Controls (*n*=11)	**LTLE (*n*=14)**	**RTLE (*n*=10)**	**Control vs. LTLE vs. RTLE**	**Control vs. LTLE**	**Control vs. RTLE**
Gender (M)	6	3	5	0.18[a]	0.12[d]	>0.99[d]
Handedness (right)	9	13	9	0.68[a]	0.56[d]	>0.99[d]
Age (years, mean+SD)	34.7+7.8	35.1+12.8	41.6+12.2	0.10[b]	0.85[c]	0.09[c]
Education (years, mean+SD)	15.6+3.2	14.4+1.7	12.5+2.7	0.26[b]	0.55[c]	0.08[c]
Epilepsy duration (years, mean+SD)	–	14.5+16.1	30.8+19.9	0.06[c]	–	–

[*] Significant at 0.05 level of significance.

[a] Chi-square test.

[b] Kruskal–Wallis test.

[c] Mann-Whitney *U* test.

[d] Fisher exact test.

Table 2

Baseline characteristics of temporal lobe epilepsy patients.

Laterality	Age	Sex	Race	Education (y)	Handedness	Epilepsy duration (y)	EEG	MRI
L	33	F	As	14	Right	16	LT sp.	L MTS
L	23	F	C	14	Right	4	LT sp.	L MT fullness (cortical dysplasia/ neoplasm)
L	22	F	C	13	Right	4	LT slowing	Normal
L	67	F	Other	NA	Right	64	BT sp.	L MTS
L	22	M	AA	12	Right	5	L F–T sp.	Decreased volume and signal abnormality of splenium CC
L	23	F	H	16	Right	11	LT sp, LF > RF sp.	L MT fullness (cortical dysplasia/ neoplasm)
L	39	F	AA	15	Right	27	LT > RT sp.	Subtle LT increased signal
L	32	M	H	13	Right	17	LT sp.	Normal
L	38	F	AA	12	Right	6	LT sp.	L MT increased signal/fullness
L	37	F	H	NA	Right	22	BT/ bifrontal sp.	Bilateral hippocampal sclerosis
L	42	F	AA	NA	Right	9	LT sp.	L cortical dysplasia
L	33	F	C	16	Right	11	LT sp.	L cortical dysplasia
L	28	M	C	17	Left	1	LT sp.	Normal
L	53	F	C	16	Right	7	LT sp.	L fullness
R	38	F	H	9	Right	32	RT sp.	R MTS
R	61	F	H	9	Right	56	RT sp.	R MTS
R	56	M	AA	12	Right	56	RT sp.	Asymmetric enlargement of right temporal horn—R hippocampal atrophy
R	43	F	C	NA	Right	40	RT > bifrontal sp.	Possible R hippocampal atrophy/ signal change
R	47	F	H	16	Right	3	RT > LT sp.	R MTS
R	36	M	C	12	Left	30	RT sp.	Mild generalized parenchymal volume loss, right cerebellar infarcts
R	21	M	Other	NA	Right	9	RT sp.	Normal

Laterality	Age	Sex	Race	Education (y)	Handedness	Epilepsy duration (y)	EEG	MRI
R	28	M	AA	12	Right	4	NA	R hippocampal fullness and increased signal
R	37	M	C	16	Right	27	RT > LT sp.	R Cavernous malformation
R	49	F	H	14	Right	49	RT sp.	R hippocampal increased signal and volume loss, L MT increased signal

Abbreviations: L, left; R, right; F, female; M, male; As, Asian; AA, African–American; H, Hispanic; C, Caucasian; sp, spikes; LT, left temporal; BT, bitemporal; RT, right temporal; MTS, mesial temporal sclerosis; MT, mesial temporal; y, years.

Table 3

Variables selected by elastic net (EN) as associated with SC–FC coupling, among all TLE patients. Variables selected by > 50% of EN cross-validation runs are shown. Measures of both functional (BC, LE, CC) and structural integrity (FA, MD) were assessed.

Region/metric	Structural/functional	VIP	EN regression coefficient (mean, 95% confidence interval)
PCG L (CC)	Functional	0.595	−0.1026 (−0.1969, −0.0272)
PCG R (BC)	Functional	0.595	+0.0861 (0.0213, 0.1339)
HIP L (BC)	Functional	0.586	+0.0809 (0.0362, 0.1024)
PCG L (LE)	Functional	0.586	−0.0663 (−0.1219, −0.0162)
HIP R (CC)	Functional	0.576	−0.1045 (−0.1612, −0.0168)
HIP R (FA)	Structural	0.576	−0.0731 (−0.1083, −0.0163)
PCG R (LE)	Functional	0.561	−0.0303 (−0.0583, −0.0023)
FIOG L (FA)	Structural	0.523	−0.1292 (−0.2591, −0.0104)

Abbreviations: VIP, variable inclusion probability; EN, elastic net; PCG, posterior cingulate gyrus; HIP, hippocampus; FIOG, frontal inferior orbital gyrus; L, left; R, right; CC, clustering coefficient; BC, betweenness centrality; LE, local efficiency; FA, fractional anisotropy.

Table 4

Variables selected by elastic net (EN) as associated with SC–FC coupling, for left and right TLE subgroups. Variables selected by 450% of EN cross-validation runs are shown. Directionality of the association of each regional measure with increased SC–FC coupling is indicated by the sign of the EN regression coefficient. Correlations with epilepsy duration and corresponding p-values are also shown. Asterisks denote variables significantly correlated with epilepsy duration at 0.05 level. Measures of both functional (BC, LE, CC) and structural integrity (FA, MD) were assessed.

Region/metric	Structural/ functional	VIP	EN regression coefficient (mean, 95% confidence interval)	Correlation with epilepsy duration	*p*-Value for correlation with epilepsy duration
			Left TLE		
FUS R (FA)	Structural	0.904	−0.192 (−0.2957, −0.0469)	−0.66	0.01*
PCG L (LE)	Functional	0.904	−0.0795 (−0.0995, −0.0336)	−0.17	0.57
PCG R (LE)	Functional	0.896	−0.0945 (−0.19, −0.0144)	−0.18	0.55
PCG R (BC)	Functional	0.876	0.1061 (0.0224, 0.1973)	+0.22	0.48
FIOG L (MD)	Structural	0.876	0.0774 (0.0286, 0.1027)	+0.63	0.02*
PCG L (CC)	Functional	0.834	−0.0615 (−0.0809, −0.0064)	−0.22	0.47
FIOG L (FA)	Structural	0.733	−0.1335 (−0.2316, −0.0262)	−0.35	0.25
CAU L (MD)	Structural	0.607	0.0212 (0.0024, 0.0278)	+0.23	0.43
ACG L (BC)	Functional	0.508	0.0898 (0.0053, 0.1552)	+0.54	0.05
PCG R (CC)	Functional	0.508	− 0.0597 (− 0.1342, −0.0014)	−0.07	0.80
	Right TLE				
HIP L (BC)	Functional	0.847	0.1485 (0.0429, 0.2036)	+0.80	0.02*
HIP R (BC)	Functional	0.807	0.1012 (0.003, 0.2179)	+0.81	0.01*
HIP R (CC)	Functional	0.557	− 0.0495 (− 0.0897, −0.0067)	−0.66	0.08

Abbreviations: VIP, variable inclusion probability; EN, elastic net; FUS, fusiform gyrus; PCG, posterior cingulate gyrus; FIOG, frontal inferior orbital gyrus; CAU, caudate; ACG, anterior cingulate gyrus; HIP, hippocampus; L, left; R, right; FA, fractional anisotropy; LE, local efficiency; BC, betweenness centrality; CC, clustering coefficient; MD, mean diffusivity.